Supplementary Materials:

Supplementary methods:

Shedding episode analysis. We defined a single episode as a series of HSV-positive swabs with two negative swabs before and after. We discarded episodes where swabs were more than 12 h apart (i.e. 2 or more consecutive missing samples) and classified episodes as short (0 - 1 day), medium (1-2 days) and long (>2 d). For each episode, we quantified first peak viral load, viral load at the first positive swab, time to first episode peak and episode duration. Often episodes had multiple peaks (Fig 1a). The first peak was defined as the highest viral load preceding any decrease in viral load during the episode. Episode analysis and visualization were performed in R (1).

Image analysis of human biopsy specimens. We focused our analysis on CD8+ and CD4+ T cells in close proximity to the dermal-epidermal junction (DEJ), cropping all areas below the DEJ that were more than half the thickness of the epidermis below the dermal-epidermal junction. This was necessary because both the neurons and the CD4+ T cells register in the green channel of the images with the former potentially distorting the CD4+ counts. These cut areas typically had high neuronal density and low nuclear density.

Using a custom R script, we used the output from Cell Profiler for each image to analyze clustering of CD8+ and CD4+T cells and to calculate E:T (effector : target) ratios for CD8+ T cells alone, CD4+ T cells alone, and all T cells within micro-regions from the biopsy. We started by dividing the image into micro-regions containing approximately 100 cells by performing k-means clustering on the positions of cell nuclei. We then assigned each CD8+ or CD4+ T cell to a micro-region by determining which cluster centroid was closest to each T cell **(Fig. 2b, c)**. Finally we computed E:T ratios for each 100-total cell cluster and for the biopsy overall.

Individual-based model of viral spread and immunological containment of infection by T_{RM}. We developed a stochastic, agent-based, spatially explicit model of HSV infection that incorporates key features of host and virus life cycles and immune control by CD8+ and CD4+ T cells. The model was run on a 2D grid of sites; each site on the L x L grid is either vacant (no cell, no virus) or occupied by a single epithelial cell and one or more virus particles. In addition, each site may be patrolled by a resident memory T cell (T_{RM}) that is either HSV-specific or a bystander in the context of HSV infection. The size of the grid (L) ranged between 125x125 and 425x425 depending on the simulation.

At each site, we tracked the state of the epithelial cell, the state of any T_{RM} patrolling the site, the number of infectious viruses present, and the concentration of cytokines at the site. At the start of the simulation, all sites were occupied by susceptible cells and a lawn of T cells at a pre-defined spatial density (defined as the probability that the focal site at the center of the grid contains T_{RM}). State transitions occurred stochastically at probabilities that were determined by the rates of various events that can occur at the site described below (70). These rates determined the wait time, a random variable whose mean is the reciprocal of the corresponding rate. Particle decay rate and cell decay rate were stochastically drawn from an exponential distribution at each site and time step. To avoid doubly propagating the particles or adding any dependency on order of cell evaluation, the value of decay for each cell and particle were generated before these

values were applied at the end of each time step. Diffusion was based on a gaussian spread over a given range based on input diffusion rates.

For all simulations involving model fitting, we populated the grid with a spatial distribution of T_{RM} drawn from the histologic slides from 10 participants in the human biopsy study described above (**Fig. 2a**). The E:T ratios from the image analysis above were used to generate rank order distributions of ratios for each biopsy and fit to an exponential curve of the form E:T ratio = $p*e^{c*rank}$. Fits of the exponential model to the 18 rank abundance curves were as follows: median R^2 =0.91 and range = 0.62-0.94. The resulting distributions of the coefficients p and c were used when seeding clusters of 100 cells in the simulated cell grid prior to each simulated episode.

Each susceptible cell at site (i, j) were infected at rate βV_{ij}, where β was viral infectivity, and V_{ij} the number of viruses present at the site. Newly infected cells entered an eclipse phase during which they did not produce virus and then transitioned at rate ε to a virus-producing state, producing μ free virus per unit time. Productively infected cells died at rate δ_I, while susceptible cells and pre-productively infected cells died at rate δ_S. Vacant sites and sites occupied by dead cells are repopulated by susceptible cells at rate α. Unless otherwise noted **(Fig S2)**, each simulation started with a single productively infected cell placed at the center of the grid and populations were recorded at 10-minute increments of simulated time for 5 days. Cell and virus parameters are listed in **Table S1**.

To this basic version of viral spread, we added immune mechanisms with features that can be switched on or off depending on the hypothesis being tested. When T_{RM} were present, they patrolled the grid at a specified rate. Movement could occur by either a "random walk", i.e. taking one step in a random direction within a 3 x 3 Moore neighborhood at a specified rate; "Levy walk", a modified random walk where step size is drawn from a Levy distribution (71); or "directed walk" where the T cell moves preferentially along a cytokine gradient (if present) and towards an infected cell when present within a 5 x 5 Moore neighborhood. For most simulations, unless specified, we assumed a random walk. T cell parameters are listed in **Table S2**.

Given that class MHC I complexes expressing HSV-peptide on infected keratinocytes are recognized by CD8+ T cells, we assumed HSV-specificity among this cell subset. When an HSV-specific CD8+ T_{RM} encountered an infected cell, movement stopped and the T cell did one or more of the following: proliferate, kill the infected cell, and/or secrete cytokines. Rates of each of these processes were determined from the literature or inferred by fitting to data **(Tables S2 and S3)**. The dendritic shape of T_{RM} was modelled by allowing HSV-specific T_{RM} to recognize and kill an infected cell within a 3 x 3 Moore neighborhood of its current position. *In situ* T cell proliferation was modeled by placing a daughter T cell at a randomly chosen vacant site within a 3 x 3 Moore neighborhood of the focal cell.

When activated, both HSV-2 specific and bystander T cells were assumed to secrete cytokines at a defined rate and cytokines could then diffuse rapidly across the grid. When present at a site containing a keratinocyte, cytokines had multiple possible concentration-dependent effects including reducing infectivity of virus to susceptible cells, reducing viral replication rate in infected cells, and decreasing lifespan of infected cells. In addition, cytokines could activate bystander T cells that were not specific for HSV, allowing them to amplify the cytokine-mediated signal. Cytokine-related parameters are listed in **Table S3**. Cytokine effects (decreased viral replication, increased cell death rate, decreased viral infectivity and increased activation of surrounding T_{RM}) were modeled with the following pharmacodynamic equation:

$$\text{effect} = \frac{1}{1 + \frac{dose}{IC50}}$$

in which dose is the cytokine level (in pg/ml) within the single-cell region and IC50 is the level of cytokine required to achieve half-maximal effect. The product is then multiplied by the parameter of relevance.

Statistics: model fitting to data. We initially fit the model without T_{RM} to achieve realistically high viral loads after 24 hours of shedding. Using a search algorithm and predefined ranges from the literature **(Table 1)**, we tuned parameters of HSV-2 infectivity rate and diffusion rate, while fixing values for viral replication rate and clearance rate at experimentally observed values. We also tuned the model to diameter of the infected cell region from the empirical data. Simulated ulcer diameter was calculated from the number of dead cells (2, 3).

In order to evaluate models with and without various cytokine effects, we used a fixed set of viral and T_{RM} parameters and varied only the parameters associated with each of the four cytokine effects. Parameter sets that did not yield at least one large episode were discarded. A large episode was defined as generating the equivalent of a 1.0 mm diameter ulcer. We fit each model to the rank order distributions of the collected cohort data described above (**Fig. 1**) for first episode peak viral load, time to first peak and duration. The residual sum of squares (RSS) was calculated by comparing the ranked values for the cohort data with ranked values for the simulated episodes. The squared error at each point was divided by the mean of the cohort measure in order to standardize the results across the different variables. The overall AIC score was calculated using the RSS score for each category together with a complexity variable "k" that differed for each model based on the number of free parameters it introduced and a shared *n* value that represented the number of data fitting points in each of the three rankings. The *n* value was 83 based on the cohort episode count. Decreasing E:T ratios below 0.15 and, to a lesser extent, increasing the number of infectious plaques allowed higher first peak viral loads and numbers of infected cells (Fig S2). parameter set yielded less than that number of episodes in 125 attempts, then it was discarded. Each attempt started with one infected cell at the center of the grid. The equation used is shown below.

$$AIC = n\left(\ln\frac{RSS_{peak}}{n} + \ln\frac{RSS_{time\ to\ peak}}{n} + \ln\frac{RSS_{duration}}{n}\right) + 2k$$

The baseline model had no cytokine effects and was assigned a *k* value of zero. The median and range of the 10 lowest AIC scores from parameter combinations for each of the 16 models was used to determine the best fit model (**Fig. S1a)**.

The final best parameter set from the initial fitting and fine-tuning exercise is shown in **Table 3**. Once the best parameters were estimated for each model, we ran 100 simulations with those parameters with 83 episodes each to average out any stochastic effects before determining the best model according to median and range of AIC scores **(Fig S1)**.

Modeling CD4+ T cells. We modeled the CD4+ T cells as behaving like bystander CD8+ T cells in that they could not recognize HSV infected cells directly but could propagate cytokine signals and hence participate in protecting susceptible cells and in hastening the death of infected cells. When seeding the simulated cell matrix with T cells, we used E:T ratios that included both cell types, but calculated percent HSV-2 specificity for CD8+ T cells alone. We used this highest reported HSV-specific ratio in order to bias towards control despite the low T cell densities **(Fig 4)**.

In silico knock-out analyses. We ran simulations to evaluate the effect of removing single functions from the model and then measured results against the following metrics of episode severity: first peak viral load, time to first peak viral load, duration and total number of infected cells. Simulated sampling was every 6 hours to align with the cohort data in these model projections. Starting with the best parameter set for the full cytokine effects model, we ran additional simulations of 100 episodes each in which we removed one or more cytokine effects or T_{RM} features. These 100 episodes were run with a random distribution of T_{RM} density as per **Fig 2**. The cytokine effects removed were reduction in viral infectivity, viral production, acceleration of infected cell death and T_{RM} activation. The latter was split into cytokine-modulated production of cytokine from bystander T_{RM} and cytokine-modulated activation of both HSV-specific and bystander T_{RM}. The T_{RM} effects included reducing dendricity, halting mobility, lowering *in situ* proliferation, and eliminating contact-mediated killing by HSV-specific T_{RM}.

T_{EM} mathematical model. As a comparator model to our models above, which assume pre-existing T_{RM} which may or may not exert certain cytokine or non-cytokine mediated functions depending on the model, we created a model without T_{RM} and rather assumed that all T cells involved in containing local HSV-2 arrive randomly from blood. To estimate the possible number of T cells that might arrive at a given micro-environment per minute, we made the following estimate: cardiac output (~6 L / day) * 1000 mL/L * proportion of cardiac output to skin capillaries (0.01) (4) * ratio of genital skin to total skin (0.01) (5)* proportion of total genital skin infected (0.01) * (1/24 days/hours) to estimate blood flow to each micro-region per hour $2.5*10^{-4}$ ml/hour. There are $2*10^{6}$ lymphocytes per mL of blood, ~30% of which are CD8+ T cells and 1% of which are HSV-2 specific (6). This leads to an estimate of 1.5 HSV-2 specific cells traveling through infected tissue per hour. However, the dwell time of lymphocytes in tissues in unknown and most of the above values are prone to enormous uncertainty and variability from person-to-person. We therefore tested the model for a broad range of T_{EM} infusion rates to the infected site with an assumed dwell time in tissue of 30 minutes. Despite a higher proportion of rapidly contained episodes with higher T_{EM} infusion rates, none of these rates provided good model fit to the data.

Supplementary figures:

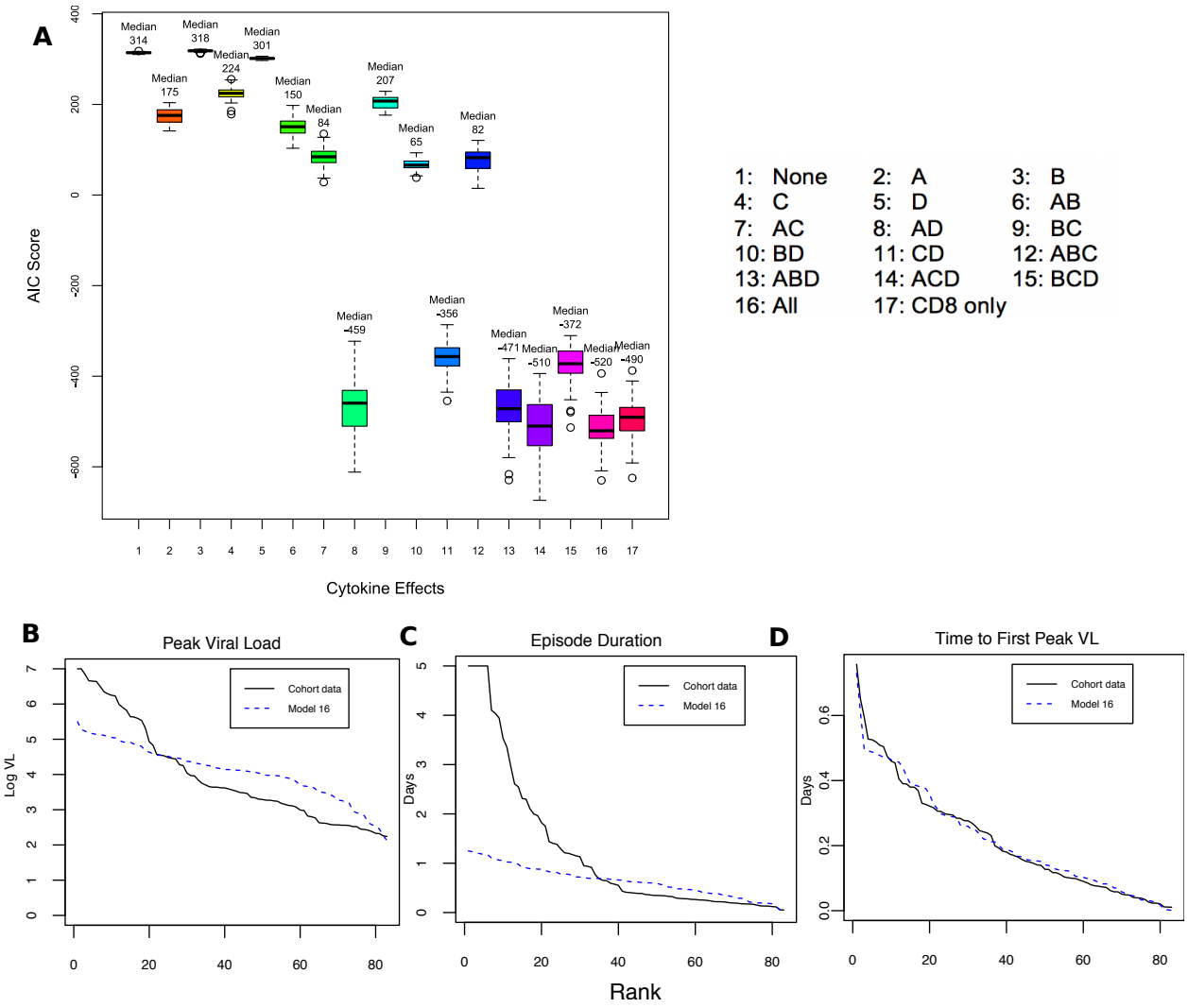

Fig. S1. Optimal fit to the data with a mathematical model including multiple antiviral cytokine functions. (A) Optimized AIC scores for models including and excluding various possible cytokine functions including: A, increasing infected cell death rate; B, decreasing viral infectivity; C, lowering viral replication rate in infected cells; and D, activating other bystander T_{RM} by increasing their proliferation and secretion of cytokines; low AIC scores represent higher likelihood models; lowest AIC scores occur with the most inclusive model; boxplots = interquartile ranges (IQR) and whiskers = ranges or 1.5x the IQR for 100 simulations of each model with optimized parameters and 83 episodes per simulation. **(B-D)** Rank abundance curves of 83 episodes sorted from highest to lowest according to episode **(B)** peak viral loads, **(C)** duration and **(D)** time to peak viral load; black lines = episode data and blue lines = optimized values from the mathematical model.

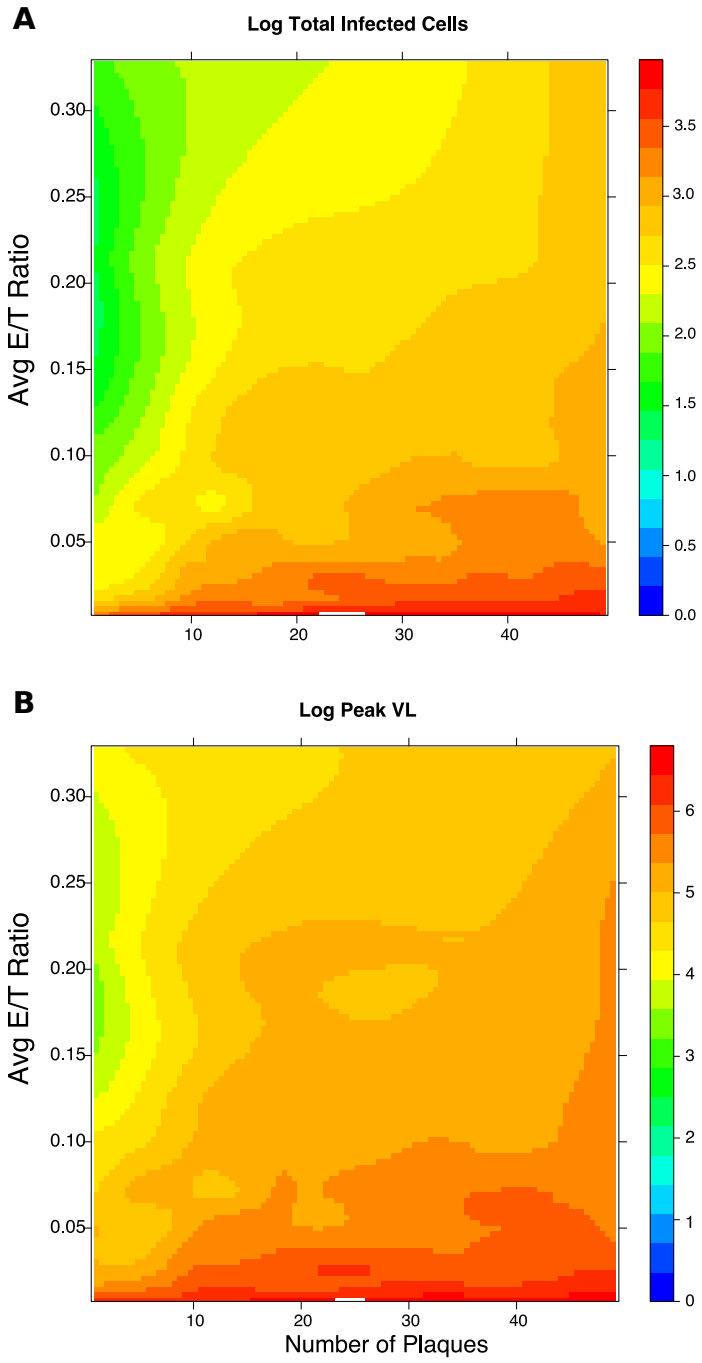

Fig. S2. Influence of T_{RM} density and initial number of infected cells on shedding episode severity. Results from 1000 simulations in which number of seeded initial infected cells evenly distributed across the entire simulated field (x-axis) and T_{RM} density E:T ratio (y-axis) were varied. **(A)** In the top panel, the heat map shows log10 number of infected cells per episode. **(B)** In the bottom panel, the heat map shows log10 peak viral load during the episode. Small decreases in E:T ratio allow more severe episodes.

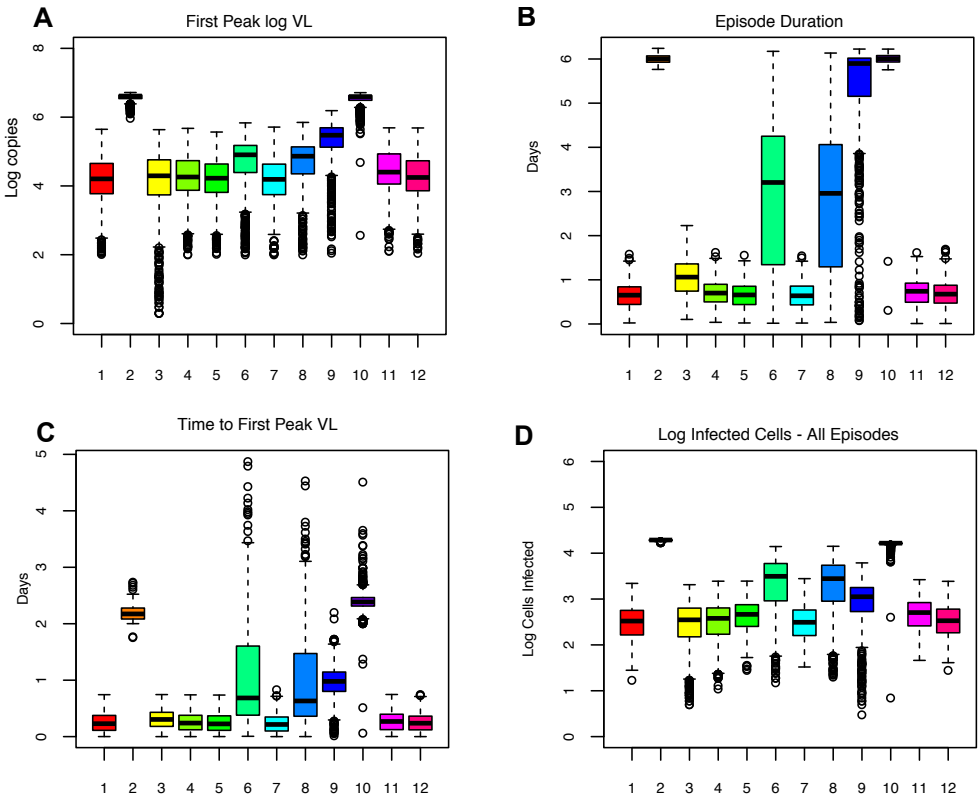

1: Baseline Best model from the 16 model comparison
2: Best model minus all cytokine effects
3: Best model minus cytokine effect on infected cell lifespan
4: Best model minus cytokine effect on viral reproduction rate
5: Best model minus cytokine effect on viral infectivity
6: Best model minus cytokine effect on TRM activation (proliferation & cytokine production)
7: Best model minus cytokine effect on TRM activation (proliferation only)
8: Best model minus cytokine effect on TRM activation (cytokine only)
9: Best model minus cytokine effect on infected cell lifespan & viral reproduction rate
10: Best model minus cytokine effect on infected cell lifespan, viral reproduction rate & TRM activation (proliferation & cytokine production)
11: Best model minus cytokine effect on infected cell lifespan, viral infectivity & TRM activation (proliferation & cytokine production)
12: Best model minus cytokine effect on viral infectivity, viral reproduction rate & TRM activation (proliferation & cytokine production)

Fig. S3. *in silico* knock out experiments of individual T_{RM} cytokine functions on HSV-2 episode severity. Episodes simulated with starting CD4+ and CD8+ T_{RM} E:T ratio densities randomly selected from **Fig. 2d** under conditions in which cytokine effects were limited to one or more of the following mechanisms: enhancing infected cell death rate, decreasing viral replication rate in infected cells, decreasing infectivity to uninfected cells and activating local bystander T_{RM}; one thousand episodes simulated per model; model descriptions below the figure; episode severity measured according to **(A)** log10 peak viral load, **(B)** duration, **(C)** time to peak viral load and **(D)** log10 total number of infected cells by 5 days; results displayed with histograms showing median, interquartile range box, values within 1.5 of the IQR (whiskers) and individual episodes (dots); models with removal of certain single cytokine effects continue to allow rapid control of most episodes but lowering infected cell lifespan and activating bystander T_{RM} are vital for control of most episodes.

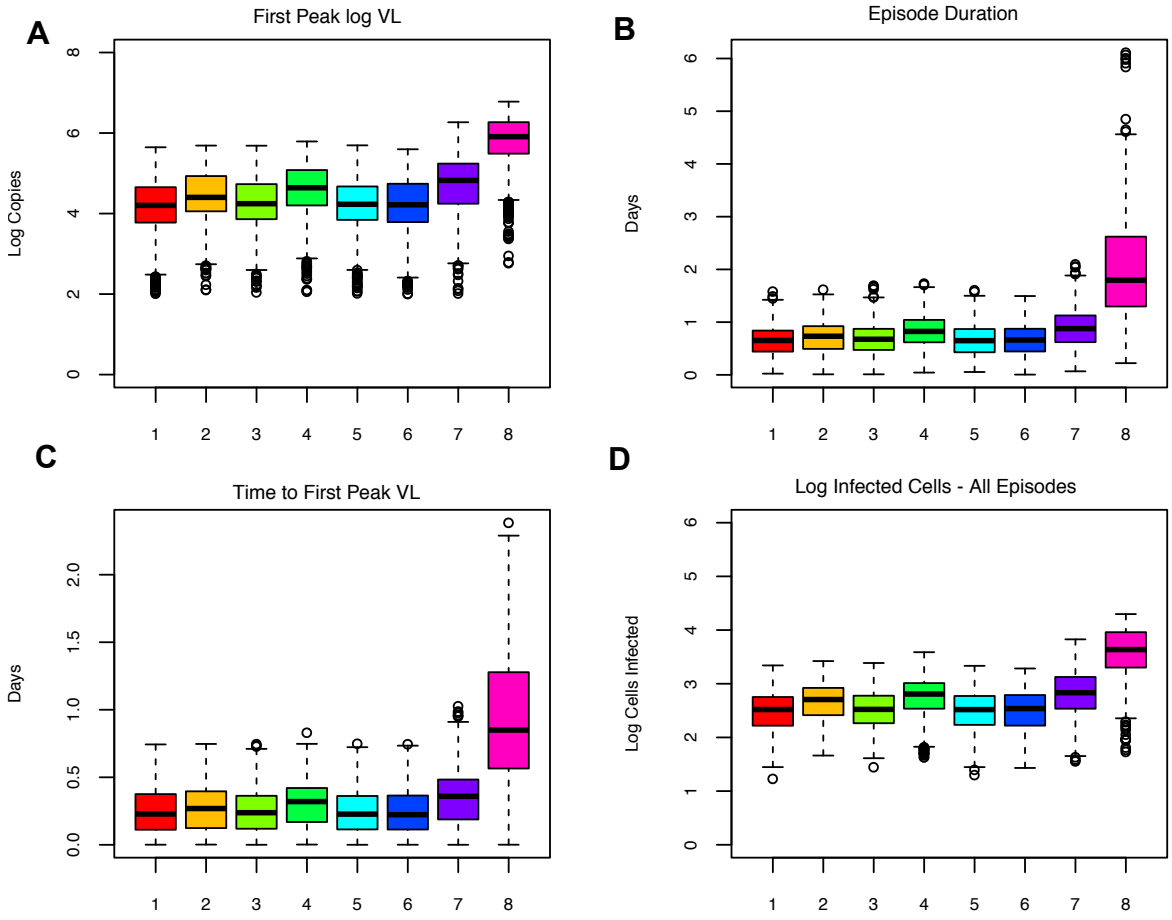

1: Baseline Best model from 16 model comparisons
2: Best model minus Trm dendricity
3: Best model minus Trm mobility
4: Best model minus Trm dendricity & mobility
5: Best model minus Trm mediated contact killing
6: Best model minus Trm replication
7: Best model with 10% HSV-specific CD8+ T cells
8: Best model with 1% HSV-specific CD8+ T cells

Fig. S4. *in silico* knock out experiments of individual T_{RM} non-cytokine functions on HSV-2 episode severity. Episodes simulated with starting CD4+ and CD8+ T_{RM} E:T ratio densities randomly selected from **Fig. 2d** under conditions in which T_{RM} dendricity, proliferation, trafficking or contact-mediated killing is absent; additional simulations assume lower proportions of HSV-2 specific CD8+ $T_{RM;}$ 1000 episodes simulated per model; model descriptions below the figure; episode severity measured according to **(A)** log10 peak viral load, **(B)** duration, **(C)** time to peak viral load and **(D)** log10 total number of infected cells by 5 days; results displayed with histograms showing median, interquartile range box, values within 1.5 of the IQR (whiskers) and individual episodes (dots). Only lowering the percentage of HSV-2 specific CD8+ T_{RM} leads to more severe episodes overall.

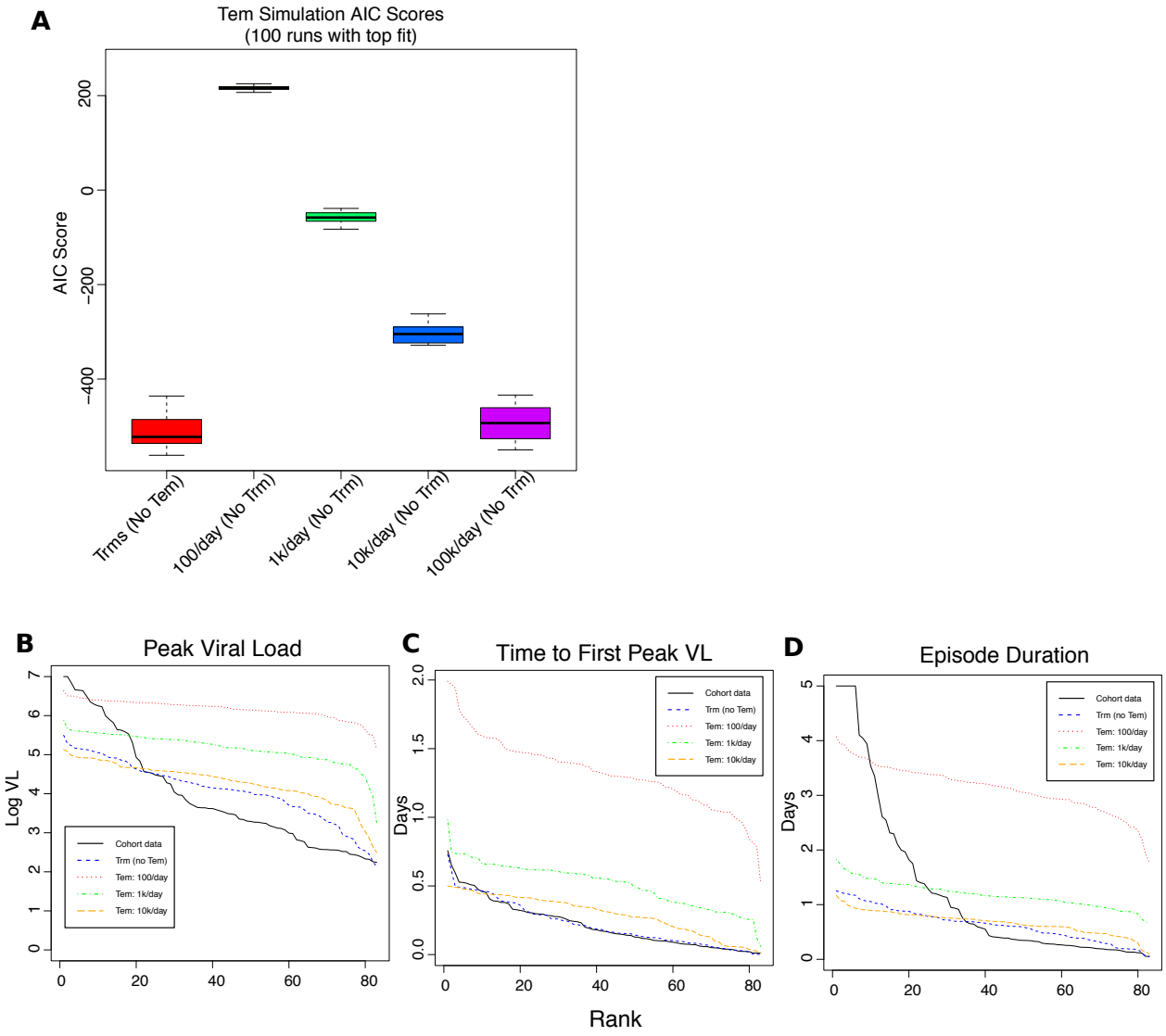

Fig. S5. Poor fit to data with a model including trafficking of T cells via blood to infected tissue rather than pre-existing T_{RM}. (A-B) Rank abundance curves of 83 episodes sorted from highest to lowest according to episode **(B)** first peak viral loads, **(C)** duration and **(D)** time to peak viral load; black lines = episode data and colored lines = models with different rates of T cell infusion (10, 100, 1000, 10000 and 100000 per day). While infused effector T cells can induce protection at high enough numbers, they do not produce sufficient heterogeneity in episode severity to allow model fit.

Movies: All movies are available for download via the following link:
https://doi.org/10.5281/zenodo.3369320

Movie S1. Lack of containment of HSV-2 spread in the absence of T_{RM}. One simulated episode on a large cell field. Left panel: ulcer cell dynamics with cell counts in the legend, peach= uninfected cells, green = pre-productive infection, red = productive infection, black = virally lysed cell. Right panel: Viral loads (HSV DNA copies) per cellular region: purple=10^{2}-$10^{2.25}$, blue=$10^{2.25}$-$10^{2.5}$, green=$10^{2.5}$-$10^{2.75}$, yellow=$10^{2.75}$-10^{3}, orange=10^{3}-$10^{3.25}$, red=$10^{3.25}$-$10^{3.5}$, dark red>$10^{3.5}$.

Movie S2. Lack of containment of HSV-2 spread in the presence of T_{RM} which only kill via direct lysis of infected cells (large field). One simulated episode on a large cell field. Left panel: ulcer cell dynamics with cell counts in the legend, peach= uninfected cells, green = pre-productive infection, red = productive infection, black = virally lysed cell, purple=T_{RM} lysed cell. Middle panel: viral loads (HSV DNA copies) per cellular region: purple=10^{2}-$10^{2.25}$, blue=$10^{2.25}$-$10^{2.5}$, green=$10^{2.5}$-$10^{2.75}$, yellow=$10^{2.75}$-10^{3}, orange=10^{3}-$10^{3.25}$, red=$10^{3.25}$-$10^{3.5}$, dark red>$10^{3.5}$. Right panel: tissue-resident T cell dynamics with cell counts in the legend, green = inactivated HSV-specific T_{RM}, red = activated HSV-specific T_{RM}, blue = inactivated bystander T_{RM}, purple = activated bystander T_{RM}.

Movie S3. Lack of containment of HSV-2 spread in the presence of T_{RM} which only kill via direct lysis of infected cells (small field). One simulated episode on a small cell field. Left panel: ulcer cell dynamics with cell counts in the legend, peach= uninfected cells, green = pre-productive infection, red = productive infection, black = virally lysed cell, purple=T_{RM} lysed cell. Middle panel: viral loads (HSV DNA copies) per cellular region: purple=10^{2}-$10^{2.25}$, blue=$10^{2.25}$-$10^{2.5}$, green=$10^{2.5}$-$10^{2.75}$, yellow=$10^{2.75}$-10^{3}, orange=10^{3}-$10^{3.25}$, red=$10^{3.25}$-$10^{3.5}$, dark red>$10^{3.5}$. Right panel: tissue-resident T cell dynamics with cell counts in the legend, green = inactivated HSV-specific T_{RM}, red = activated HSV-specific T_{RM}, blue = inactivated bystander T_{RM}, purple = activated bystander T_{RM}.

Movie S4. Rapid containment of HSV-2 spread in the presence of T_{RM} antiviral cytokine secretion and high T_{RM} density. Four simulated episodes with high initial T_{RM} density leading to rapid control of infection on a small cell field. Left upper panel: ulcer cell dynamics with cell counts in the legend, peach= uninfected cells, green = pre-productive infection, red = productive infection, black = virally lysed cell, purple=T_{RM} lysed cell, grey=cytokine lysed cell. Right upper panel: viral loads (HSV DNA copies) per cellular region: purple=10^{2}-$10^{2.25}$, blue=$10^{2.25}$-$10^{2.5}$, green=$10^{2.5}$-$10^{2.75}$, yellow=$10^{2.75}$-10^{3}, orange=10^{3}-$10^{3.25}$, red=$10^{3.25}$-$10^{3.5}$, dark red>$10^{3.5}$. Left lower panel: tissue-resident T cell dynamics with cell counts in the legend, green = inactivated HSV-specific T_{RM}, red = activated HSV-specific T_{RM}, blue = inactivated bystander T_{RM}, purple = activated bystander T_{RM}. Right lower panel = concentration of cytokine indicated by darkness of color; red is over infected cells or dead cells, indicating limitation of viral replication and infected cell lifespan; blue is over uninfected cells, indicating limitation of new infection.

Movie S5. Containment of HSV-2 spread in the presence of T_{RM} antiviral cytokine secretion and low T_{RM} density (small field). Four simulated episodes on a small cell field with low initial T_{RM} density leading to slower control of infection. Left upper panel: ulcer cell

dynamics with cell counts in the legend, peach= uninfected cells, green = pre-productive infection, red = productive infection, black = virally lysed cell, purple=T_{RM} lysed cell, grey=cytokine lysed cell. Right upper panel: viral loads (HSV DNA copies) per cellular region: purple=10^{2}-$10^{2.25}$, blue=$10^{2.25}$-$10^{2.5}$, green=$10^{2.5}$-$10^{2.75}$, yellow=$10^{2.75}$-10^{3}, orange=10^{3}-$10^{3.25}$, red=$10^{3.25}$-$10^{3.5}$, dark red>$10^{3.5}$. Left lower panel: tissue-resident T cell dynamics with cell counts in the legend, green = inactivated HSV-specific T_{RM}, red = activated HSV-specific T_{RM}, blue = inactivated bystander $T_{RM,}$ purple = activated bystander T_{RM}. Right lower panel = concentration of cytokine indicated by darkness of color; red is over infected cells or dead cells, indicating limitation of viral replication and infected cell lifespan; blue is over uninfected cells, indicating limitation of new infection.

Movie S6. Containment of HSV-2 spread in the presence of T_{RM} antiviral cytokine secretion and low T_{RM} density (large field). A simulated episode on a large cell field with low initial T_{RM} density leading to slower control of infection. Left upper panel: ulcer cell dynamics with cell counts in the legend, peach= uninfected cells, green = pre-productive infection, red = productive infection, black = virally lysed cell, purple=T_{RM} lysed cell, grey=cytokine lysed cell. Right upper panel: viral loads (HSV DNA copies) per cellular region: purple=10^{2}-$10^{2.25}$, blue=$10^{2.25}$-$10^{2.5}$, green=$10^{2.5}$-$10^{2.75}$, yellow=$10^{2.75}$-10^{3}, orange=10^{3}-$10^{3.25}$, red=$10^{3.25}$-$10^{3.5}$, dark red>$10^{3.5}$. Left lower panel: tissue-resident T cell dynamics with cell counts in the legend, green = inactivated HSV-specific T_{RM}, red = activated HSV-specific T_{RM}, blue = inactivated bystander $T_{RM,}$ purple = activated bystander T_{RM}. Right lower panel = concentration of cytokine indicated by darkness of color; red is over infected cells or dead cells, indicating limitation of viral replication and infected cell lifespan; blue is over uninfected cells, indicating limitation of new infection.

Movie S7. Slower containment of HSV-2 spread in the presence of T_{RM} antiviral cytokine secretion which only prevents infectivity. Four simulated episodes. Left upper panel: ulcer cell dynamics with cell counts in the legend, peach= uninfected cells, green = pre-productive infection, red = productive infection, black = virally lysed cell, purple=T_{RM} lysed cell, grey=cytokine lysed cell. Right upper panel: viral loads (HSV DNA copies) per cellular region: purple=10^{2}-$10^{2.25}$, blue=$10^{2.25}$-$10^{2.5}$, green=$10^{2.5}$-$10^{2.75}$, yellow=$10^{2.75}$-10^{3}, orange=10^{3}-$10^{3.25}$, red=$10^{3.25}$-$10^{3.5}$, dark red>$10^{3.5}$. Left lower panel: tissue-resident T cell dynamics with cell counts in the legend, green = inactivated HSV-specific T_{RM}, red = activated HSV-specific T_{RM}, blue = inactivated bystander $T_{RM,}$ purple = activated bystander T_{RM}. Right lower panel = concentration of cytokine indicated by darkness of color; blue is over uninfected cells, indicating limitation of new infection.

Movie S8. Protracted containment of HSV-2 spread in the presence of T_{RM} antiviral cytokine secretion which only limit lifespan of infected cells. Four simulated episodes. Left upper panel: ulcer cell dynamics with cell counts in the legend, peach= uninfected cells, green = pre-productive infection, red = productive infection, black = virally lysed cell, purple=T_{RM} lysed cell, grey=cytokine lysed cell. Right upper panel: viral loads (HSV DNA copies) per cellular region: purple=10^{2}-$10^{2.25}$, blue=$10^{2.25}$-$10^{2.5}$, green=$10^{2.5}$-$10^{2.75}$, yellow=$10^{2.75}$-10^{3}, orange=10^{3}-$10^{3.25}$, red=$10^{3.25}$-$10^{3.5}$, dark red>$10^{3.5}$. Left lower panel: tissue-resident T cell dynamics with cell counts in the legend, green = inactivated HSV-specific T_{RM}, red = activated HSV-specific T_{RM}, blue = inactivated bystander $T_{RM,}$ purple = activated bystander T_{RM}. Right lower panel =

concentration of cytokine indicated by darkness of color; red is over infected cells or dead cells, indicating limitation of viral replication and infected cell lifespan.

Table S1. Model parameters for cell and virus compartments in the absence of immunity

Parameter	Unit	Value	Source
Uninfected cell division rate[A] (α)	day^{-1}	0.077	(7)
Uninfected cell death rate[B] (δ_S)	day^{-1}	0	
Infected cell death rate (δ_I)	day^{-1}	1.25	(3)
Lag in virus production[C] (ε)	$cell^{-1}\ day^{-1}$	8	(8)
Infectivity rate (β)	$virus^{-1}cell^{-1}day^{-1}$	0.1	Fitted (initial model)
Virus spread rate[D]	$sites\ day^{-1}$	54	Fitted (final model)
Virus production rate (μ, mean ± SD)	$cell^{-1}\ day^{-1}$	$3.16 \pm 1.00 \times 10^4$	(3)
Free virus decay rate	$site^{-1}day^{-1}$	8.8	(9)
Spatial scale	$\mu m\ site^{-1}$	50	(10, 11)

[A] Rate at which a vacant site becomes occupied by a susceptible cell.

[B] We assumed that cell death due to infection greatly exceeds uninfected cell death during lesion formation.

[C] This rate represents the time from infection to first released virus.

[D] Rate at which infectious virus spreads across the grid.

Table S2. Tissue-resident T cell parameters.

Parameter	Unit	Value	Source
Starting density	E:T ratio	varied	**Fig 2D**
HSV-specific fraction [A]	-	0.05-0.4	(12)
Motility rate	sites day^{-1}	24	(13, 14)
Death rate[B]	day^{-1}	0	(15)
Proliferation rate upon antigen recognition	day^{-1}	3	(15, 16)
Killing rate of adjacent infected cells[C]	day^{-1}	48	(17)
Maximum number of divisions	-	5	

[A] Fraction of starting T_{RM} that are HSV-specific; remaining are bystander T_{RM}.
[B] T_{RM} death rate in the absence of antigen.
[C] This rate is applied between antigen detection to death of infected cell.

Table S3. Cytokine parameters

Parameter	Unit	Value	Source
Secretion rate by T_{RM}	pg $cell^{-1}day^{-1}$	0.02	(18)
Diffusion rate	sites day^{-1}	65	Fitted
Uptake by cells	pg $cell^{-1}day^{-1}$	6.9	Fitted
Decay rate	$site^{-1}day^{-1}$	0.01	Fitted
IC50: infected cell killing	pg $cell^{-1}$	5.4×10^{-6}	Fitted
IC50: viral infectivity	pg $cell^{-1}$	7.0×10^{-7}	Fitted
IC50: virus production	pg $cell^{-1}$	1.0×10^{-6}	Fitted
IC50: T_{RM} activation	pg $cell^{-1}$	1.6×10^{-7}	Fitted

References

1. R Core Team Vienna, Austria: R Foundation for Statistical Computing; 2015.
2. Schiffer JT, et al. Mucosal host immune response predicts the severity and duration of herpes simplex virus-2 genital tract shedding episodes. *Proc Natl Acad Sci U S A.* 2010;107(44):18973-8.
3. Schiffer JT, et al. Frequent release of low amounts of herpes simplex virus from neurons: results of a mathematical model. *Sci Transl Med.* 2009;1(7):7ra16.
4. Vroman NB, Buskirk ER, and Hodgson JL. Cardiac output and skin blood flow in lean and obese individuals during exercise in the heat. *J Appl Physiol Respir Environ Exerc Physiol.* 1983;55(1 Pt 1):69-74.
5. Pendergrass PB, Belovicz MW, and Reeves CA. Surface area of the human vagina as measured from vinyl polysiloxane casts. *Gynecol Obstet Invest.* 2003;55(2):110-3.
6. Jing L, et al. CD4 T-cell memory responses to viral infections of humans show pronounced immunodominance independent of duration or viral persistence. *J Virol.* 2013;87(5):2617-27.
7. Weinstein GD, McCullough JL, and Ross P. Cell proliferation in normal epidermis. *J Invest Dermatol.* 1984;82(6):623-8.
8. Smith JD, and De Harven E. Herpes simplex virus and human cytomegalovirus replication in WI-38 cells. I. Sequence of viral replication. *J Virol.* 1973;12(4):919-30.
9. Schiffer JT, et al. Rapid localized spread and immunologic containment define herpes simplex virus-2 reactivation in the human genital tract. *eLife.* 2013;2:e00288.
10. Brunzel NA. *Fundamentals of urine & body fluid analysis.* St. Louis, Missouri, USA: Elsevier/Saunders; 2013.
11. Evers H, Birngruber CG, Ramsthaler F, Muller U, Bruck S, and Verhoff MA. [Differentiation of epithelial cell types by cell diameter]. *Arch Kriminol.* 2011;228(1-2):11-9.
12. Zhu J, et al. Virus-specific CD8+ T cells accumulate near sensory nerve endings in genital skin during subclinical HSV-2 reactivation. *J Exp Med.* 2007;204(3):595-603.
13. Ariotti S, et al. Tissue-resident memory CD8+ T cells continuously patrol skin epithelia to quickly recognize local antigen. *Proc Natl Acad Sci U S A.* 2012;109(48):19739-44.
14. Zaid A, et al. Persistence of skin-resident memory T cells within an epidermal niche. *Proc Natl Acad Sci U S A.* 2014;111(14):5307-12.
15. De Boer RJ, Oprea M, Antia R, Murali-Krishna K, Ahmed R, and Perelson AS. Recruitment times, proliferation, and apoptosis rates during the CD8(+) T-cell response to lymphocytic choriomeningitis virus. *J Virol.* 2001;75(22):10663-9.
16. Lenardo M, et al. Mature T lymphocyte apoptosis--immune regulation in a dynamic and unpredictable antigenic environment. *Annu Rev Immunol.* 1999;17:221-53.
17. Halle S, et al. In vivo killing capacity of cytotoxic T cells is limited and involves dynamic interactions and T cell cooperativity. *Immunity.* 2016;44(2):233-45.
18. Wigginton JE, and Kirschner D. A model to predict cell-mediated immune regulatory mechanisms during human infection with Mycobacterium tuberculosis. *J Immunol.* 2001;166(3):1951-67.